Phi: Jurnal Pendidikan Fisika dan Terapan
Vol.13 No.1 (2027) 53-63
ISSN: 2460-4348, e-ISSN: 2549-7162
https://jurnal.ar-raniry.ac.id/index.php/jurnalphi/index

Article Type: *original research*

Amplitude Variation with Frequency as Direct Hydrocarbon Indicator: A Case Study from the Volve Field

Rafiki Ramadani[1*], Dinanti Syafirani Zahra[1], Eleonora Agustine[1], Ginanjar Hidayat[2]
[1]Department of Geophysics, Faculty of Mathematics and Natural Sciences, Universitas Padjadjaran, Sumedang, West Java, Indonesia
[2]Department of Center for Materials and Earth Engineering Studies, Faculty of Mathematics and Natural Sciences, Universitas Padjadjaran, Sumedang, West Java, Indonesia

Correspondence E-mail: eleonora.agustine@unpad.ac.id

ARTICLE INFO

Article History:
Received: 14 July 2026
Revised: 02 September 2026
Accepted: 03 September 2026
Published: 08 September 2026

Keywords:
Amplitude variation with frequency (AVF); Attenuation; Spectral decomposition; Post-stack seismic; Volve field;

ABSTRACT

Accurate identification of hydrocarbon-bearing zones is essential for effective reservoir characterization, particularly when pre-stack seismic data required for conventional amplitude variation with offset (AVO) analysis are limited. This study aims to evaluate the application of amplitude variation with frequency (AVF) as a direct hydrocarbon indicator (DHI) using post-stack seismic data from the Volve Field, North Sea, Norway. The analysis was performed through spectral decomposition using the Continuous Wavelet Transform (CWT) to generate frequency gathers, followed by amplitude–frequency analysis to derive Intercept and Gradient attributes. A frequency range of 5–28 Hz was selected based on the observed spectral response and used to construct the AVF product (Intercept × Gradient). The results show a high-frequency loss and a shift toward lower dominant frequencies within the hydrocarbon-bearing interval of the Hugin Formation. The AVF response is characterized by a positive Intercept and negative Gradient, resulting in negative AVF product anomalies. Validation at Wells 19-A and 19-S&SR shows that more negative AVF Product responses are associated with lower water saturation within the Hugin reservoir. Well 19-A exhibits an SW of approximately 0.203 and an AVF Product of −0.21, whereas Well 19-S&SR shows an SW of approximately 0.166 and a more negative AVF Product of −0.28. The spatial distribution of negative AVF anomalies around both validation wells further supports the delineation of hydrocarbon-prospective zones. These results indicate that AVF can provide a useful calibrated quick-look approach for hydrocarbon prospect delineation using post-stack seismic data, although integration with independent well and geological information remains essential.

This work is licensed under a Creative Commons Attribution-ShareAlike 4.0 International License

1. INTRODUCTION

Accurate identification of hydrocarbon-prospective zones is a crucial stage in oil and gas exploration and field development. One commonly used approach is Amplitude Variation with Offset (AVO) analysis, which examines changes in seismic amplitude with incidence angle (offset) as a direct indicator of hydrocarbon presence, commonly referred to as a Direct Hydrocarbon Indicator (DHI). However, the application of AVO strongly depends on the availability and quality of pre-stack seismic

data. In many field cases, such data may be unavailable, characterized by a low signal-to-noise ratio, or affected by alignment issues between seismic gathers (Mandong et al., 2021).s

The classification of gas sands by Rutherford and Williams (1989) shows that conventional AVO responses vary depending on the impedance contrast between the reservoir and the shale seal. However, in low-impedance or unconsolidated sandstone reservoirs, distinguishing hydrocarbon-bearing zones using conventional AVO responses can be ambiguous due to fluid-sensitive dispersion and attenuation (Chapman et al., 2006). When seismic waves propagate through highly attenuating media, high-frequency energy is selectively absorbed, causing the dominant frequency to shift toward lower frequencies. This frequency-dependent attenuation behavior provides an alternative basis for identifying hydrocarbon-bearing zones using seismic data (Odebeatu, 2006).

As an alternative to AVO, Amplitude Variation with Frequency (AVF) utilizes post-stack seismic data, which are generally more widely available and more robust against misalignment and random noise compared with pre-stack seismic gathers. Therefore, AVF can provide a stable and efficient quick-look indicator for reservoir delineation. The physical basis of AVF is associated with the frequency-dependent attenuation of seismic waves propagating through porous media saturated with hydrocarbon fluids. Poroelastic theory demonstrates that fluid–rock interaction and frequency-dependent dispersion in saturated porous media influence the amplitude–frequency response of seismic waves (Chapman et al., 2006; Ren et al., 2009). This behavior is further supported by physical modeling, which shows that inhomogeneous rock properties can enhance P-wave attenuation through slow-wave diffusion in hydrocarbon-bearing formations (Carcione and Picotti, 2006). Consequently, selective high-frequency attenuation and shifts in dominant frequency may provide fluid-sensitive seismic information through the AVF approach, although these responses remain non-unique and require calibration with independent reservoir information.

Before applying the AVF method to mature fields with limited data documentation, it is important to validate its performance in a field with proven hydrocarbon accumulation and reliable well control. The Volve Field, located in the North Sea, Norway, was selected as the case study in this research because it is one of the most comprehensive publicly available seismic–well datasets and has been widely used as a benchmark in exploration geophysics studies (Offshore Technology, 2020). The field contains the Hugin Formation sandstone reservoir, which has been proven to be productive and is supported by well-log data and a well-documented production history. The Hugin Formation is characterized as a clean and heavily faulted sandstone reservoir deposited in a shallow-marine and tidal setting (Pelemo-Daniels and Stewart, 2024).

The geological and geomechanical complexity of the Hugin Formation provides an appropriate setting for evaluating frequency-dependent seismic responses. Studies by Sen and Ganguli (2019) and Saha et al. (2022) provide detailed geomechanical models of the reservoir, highlighting complexities in stress profiles and pore-pressure variations. In addition, the mature nature of the Volve Field provides an opportunity to investigate reservoir changes associated with hydrocarbon depletion. Such dynamic changes can be evaluated using post-stack time-shift analysis, which has been applied to monitor changes in the subsurface during production and depletion (MacBeth et al., 2018). Furthermore, the application of frequency-dependent seismic attributes such as AVF has demonstrated promising results in other hydrocarbon fields, including the Teapot Dome Field (Rezeki et al., 2023) and the Penobscot Field (Purnomo et al., 2025). These studies support the applicability of frequency-dependent seismic analysis in both conventional and unconventional tight-sand reservoir systems.

Previous studies have demonstrated the potential of frequency-dependent seismic attributes for hydrocarbon identification; however, the quantitative calibration of post-stack AVF responses against independent reservoir-fluid indicators remains relatively limited, particularly in publicly available benchmark datasets. In addition, frequency-dependent amplitude variations in post-stack seismic data are non-unique and may also be influenced by reservoir thickness, thin-bed tuning, lithological variation, seismic bandwidth, and processing effects. Therefore, AVF anomalies should not be interpreted as direct evidence of hydrocarbon presence without independent geological and well control.

To address these limitations, this study evaluates the AVF response of the Hugin Formation in the Volve Field by integrating CWT-based spectral decomposition, amplitude–frequency

regression, water-saturation logs, and documented well information. The AVF response is calibrated using the producing Well 19-A and further evaluated at Well 19-S&SR as an additional validation well. The objectives are to characterize the frequency-dependent attenuation response of the reservoir, quantify its relationship with water saturation, and evaluate the reliability and limitations of post-stack AVF for hydrocarbon delineation.

2. METHODS

The primary dataset used in this study is 3D post-stack seismic data processed using Post-Stack Time Migration (PSTM) from the Volve Field. Well 15/9-19A (Well 19-A) was used as the primary calibration well because it penetrates the producing Hugin Formation reservoir and is supported by water saturation (SW) and production information. An additional well, 15/9-19-S&SR (Well 19-S&SR), was included as an independent validation point to evaluate whether the AVF response observed at Well 19-A is also reproduced at another reservoir location. Well reports and production information were further incorporated to support the interpretation of reservoir conditions.

The Volve Field is located in Block 15/9 in the southern Norwegian sector of the North Sea, approximately 200 km west of Stavanger and approximately 8 km from the Sleipner Ost Field, at a water depth of approximately 80 m (Offshore Technology, 2020). The field was discovered in 1993, commenced production in February 2008, and ceased production in 2016, with a total cumulative production of approximately 63 million barrels of oil (Norwegian Petroleum Directorate). The principal reservoir of the Volve Field consists of Middle Jurassic Hugin Formation sandstones, which form part of the syn-rift succession of the North Sea Basin, at a depth of approximately 2,700–3,100 m TVDSS. The reservoir structure is dome-shaped and is associated with the collapse of a salt ridge, while the western part of the structure exhibits a higher fault intensity due to salt tectonics (Szydlik et al., 2007; Sen and Ganguli, 2019). Geomechanical characterization of the Hugin Formation further indicates a strike-slip faulting regime with rock mechanical properties consistent with a moderately consolidated sandstone reservoir, providing additional structural context for the interpretation of the target interval (Saha et al., 2022). Reservoir thickness varies from approximately 20 m at the structural crest to as much as 100 m along the flanks. Regionally, the Volve Field is situated near the southern part of the Viking Graben, where a horst-graben structural configuration developed under an extensional tectonic regime. This structural setting facilitated the formation of hydrocarbon traps within the Hugin Formation reservoir.

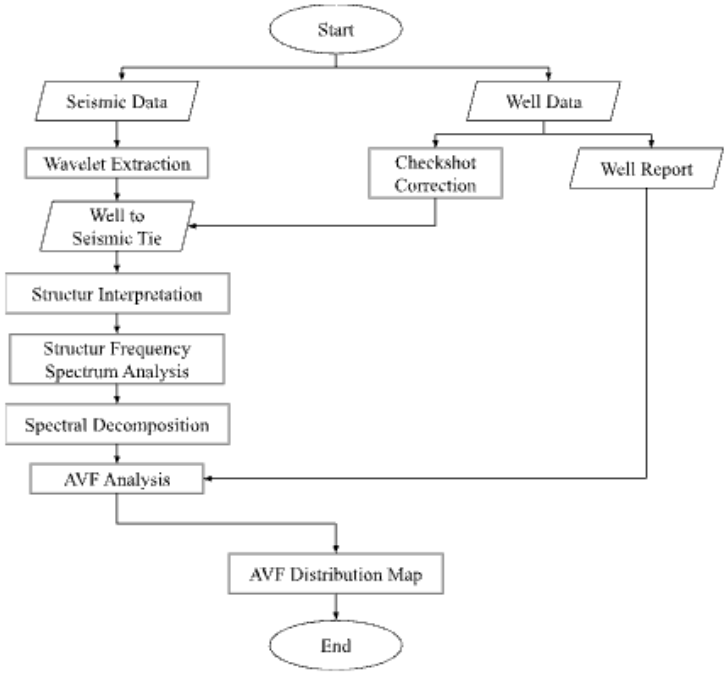


Figure 1. Research workflow of the AVF analysis from seismic and well data preparation to AVF distribution mapping.

The AVF method utilizes the phenomenon of seismic wave attenuation, namely the selective absorption of energy in the high-frequency components as seismic waves propagate through a hydrocarbon-bearing porous medium. The physical mechanism underlying this phenomenon can be explained by poroelasticity. Biot (1956) established the theoretical framework for wave propagation in fluid-saturated porous media and demonstrated that the relative motion between pore fluids and the solid rock frame produces velocity dispersion and viscous attenuation across different frequency regimes. In reservoir sandstones, seismic attenuation, commonly represented by the inverse quality factor (1/Q), can increase significantly when the pore space is partially saturated with gas. This behavior is associated with mesoscopic-scale pressure gradients and wave-induced fluid flow, in which fluids are displaced between compliant pores or fractures and the stiffer rock matrix during seismic-wave propagation (Pride et al., 2004).

The attenuation of seismic energy causes high-frequency components to be preferentially absorbed, resulting in a shift of the dominant frequency toward lower frequencies compared with non-reservoir or less attenuating rocks. This phenomenon can produce a low-frequency shadow beneath or within highly attenuating hydrocarbon-bearing reservoirs (Castagna et al., 2003). The frequency-dependent attenuation behavior therefore provides a physical basis for using AVF as a Direct Hydrocarbon Indicator (DHI). To properly characterize the elastic response of the reservoir, shear-wave velocity is also an important rock-physics parameter and can be estimated using empirical models such as the clastic silicate model of Greenberg and Castagna (1992).

Based on this attenuation principle, the AVF response can be expressed as a variation of seismic amplitude with frequency, as shown in Equation 1.

$$AVF(t) = \frac{A(f_2, t) - A(f_1, t)}{f_2 - f_1} \tag{1}$$

where $AVF(t)$ represents the amplitude at a given frequency and time, while f_1 and f_2 represent the lower and upper frequencies, respectively. More negative AVF responses indicate stronger frequency-dependent attenuation. Because similar spectral behavior may also be influenced by lithology, reservoir thickness, tuning, and seismic-data characteristics, the AVF anomaly requires independent well and geological calibration before being interpreted as hydrocarbon-related (Chen et al., 2008; Ren et al., 2009). Therefore, AVF is widely used as a quick-look method based on post-stack seismic data because it is relatively more stable against noise effects compared to pre-stack data (Mandong et al., 2021; Rezeki et al., 2023).

Spectral decomposition is a process of transforming seismic traces from the time domain into the time-frequency domain, allowing the amplitude response of seismic events to be evaluated at different frequencies. The concept of time-frequency analysis in seismic interpretation was initially demonstrated through complex-trace analysis, which enables the extraction of instantaneous envelope, phase, and frequency attributes (Tane ret al., 1979). Spectral decomposition was subsequently popularized for thin-bed reservoir delineation and stratigraphic visualization by Partyka, Gridley, and Lopez (1999).

Conventional spectral decomposition can be performed using the Short-Time Fourier Transform (STFT); however, its fixed window length creates a limitation in simultaneously achieving high time and frequency resolution. The Continuous Wavelet Transform (CWT) overcomes this limitation by using adaptive time-frequency windows, providing improved localization of frequency-dependent seismic responses (Sinha et al., 2005). In this study, CWT was therefore used for spectral decomposition because its adaptive time-frequency resolution allows localized high-frequency information, particularly that associated with thin reservoir intervals, to be preserved. Mathematically, the CWT is expressed as Equation 2.

$$W(a, \tau) = \frac{1}{\sqrt{a}} \int_{-\infty}^{\infty} s(t)\ \psi^* \left(\frac{t - \tau}{a} \right) dt \tag{2}$$

where $W(a,\tau)$ represents the wavelet coefficient,$s(t)$ is the seismic signal, ψ represent *mother wavelet*, while a represent the scale and time translation parameters, respectively. The use of CWT for spectral decomposition of seismic data follows the approach introduced by Sinha et al. (2005), who demonstrated that wavelet-based time-frequency analysis provides better resolution than conventional short-time Fourier methods for detecting frequency-dependent amplitude anomalies. A similar CWT-based spectral decomposition workflow has also been applied to delineate reservoir-quality variations in fluvial clastic systems (Naseer and Asim, 2017), supporting its reliability as a general tool for frequency-attenuation analysis across different depositional settings. In this study, the CWT was implemented using a complex Ricker mother wavelet because it provides localized time-frequency representation suitable for seismic reflection analysis. The transform was evaluated over a frequency with a frequency increment. These parameters were kept constant throughout the spectral decomposition to ensure consistent comparison of amplitude responses across the target interval.

For each seismic trace, the CWT produces a set of coefficients $W(a,b)$ representing the localized seismic response at different scales and time positions. The scale values were converted into their corresponding frequencies, and the magnitude of each coefficient, $|W(a,b)|$, was used as the amplitude representation at each time-frequency sample. These amplitudes were arranged according to frequency to construct the frequency gather. At the target reservoir time sample, the amplitude values extracted from the selected frequency components were then used to construct the amplitude-versus-frequency relationship for AVF regression. In hydrocarbon-bearing reservoirs characterized by strong attenuation, the preferential absorption of high-frequency energy can generate a shift toward lower frequencies and a low-frequency shadow, providing a measurable frequency-dependent anomaly (Castagna et al., 2003). Advanced adaptive signal decomposition techniques, such as matching pursuit using redundant time-frequency dictionaries, can also be applied to further characterize localized frequency-dependent structures (Mallat and Zhang, 1993). In this study, however, CWT-based spectral decomposition was employed to generate the frequency-domain input for AVF analysis (Mandong et al., 2021; Haryanto et al., 2022)

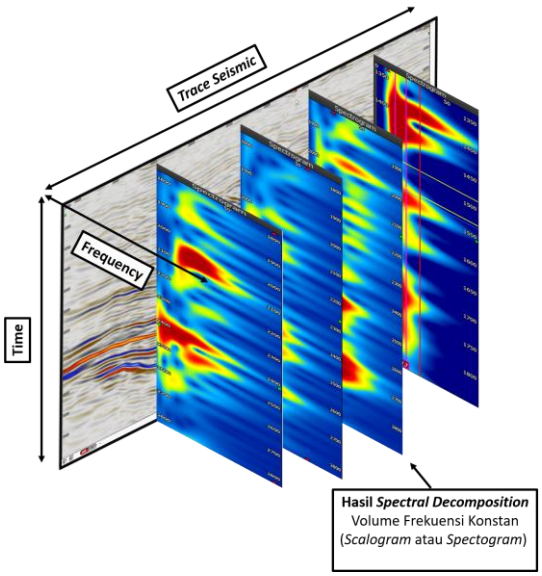


Figure 2. Illustration of a seismic trace section showing frequency variations obtained from spectral decomposition.

The frequency-dependent seismic response is also sensitive to the type and saturation of fluids occupying the reservoir pore space. Seismic reflections from anelastic and dispersive boundaries can exhibit changes in amplitude, dispersion, and dominant frequency depending on fluid saturation and reservoir properties. Odebeatu et al. (2006) demonstrated that dispersion anomalies can be mapped using spectral decomposition to distinguish gas-saturated reservoirs from brine-

saturated reservoirs. These observations provide a direct physical connection between frequency-dependent seismic behavior and hydrocarbon saturation.

The influence of fluid substitution and reservoir geometry on frequency-dependent seismic responses has also been demonstrated through reservoir modeling. Chen et al., (2008) conducted reservoir wedge modeling of deepwater reservoirs and showed that peak-frequency shifts and reflectivity changes are controlled by fluid substitution between brine, oil, and gas, as well as by reservoir thickness. Furthermore, poroelastic analysis by Ren et al., (2009) demonstrated that frequency-dependent reflection coefficients at reservoir boundaries can be used to discriminate fluid content. These findings indicate that the frequency-dependent behavior of seismic amplitude can serve as an effective indicator of hydrocarbon presence.

AVF spectrum analysis (Figure 2) was therefore performed by evaluating the variation in seismic amplitude with frequency on the frequency gather obtained from spectral decomposition. This relationship is approximated using a linear function, as presented in Equation 3,

$$A(f) = I + G(f) \tag{3}$$

where $A(f)$ represents the CWT-derived amplitude at frequency f, I is the Intercept, and G is the Gradient representing the rate of amplitude change with increasing frequency. The amplitude-frequency relationship within the selected frequency interval is approximated using linear regression. A negative Gradient therefore indicates that seismic amplitude decreases toward higher frequencies, representing a stronger frequency-dependent attenuation response (Mandong et al., 2021; Rezeki et al., 2023)

$$P = I \times G \tag{4}$$

where P represents the AVF Product. The Product combines the amplitude strength represented by the Intercept with the frequency-dependent slope represented by the Gradient. Negative Product values therefore highlight zones where a relatively strong seismic response is accompanied by decreasing amplitude toward higher frequencies. In this study, the AVF Product is interpreted as an indicator of an attenuative response and is not considered direct evidence of hydrocarbon presence without independent well validation.

The frequency interval used for AVF regression was determined from spectrum analysis at the proven hydrocarbon-bearing interval of Well 19-A and a nearby water-bearing reference interval. The two spectral responses show distinguishable amplitude behavior at lower frequencies and intersect at approximately 28 Hz, which was therefore selected as the upper cut-off frequency. The analysis was evaluated from 5 Hz, representing the lower bound of the frequency range used in the spectral comparison, to the 28 Hz intersection. Consequently, the 5–28 Hz interval was consistently applied to generate the AVF attributes.

3. RESULTS AND DISCUSSION

Spectral decomposition of the post-stack seismic data reveals a distinct difference in frequency response between the hydrocarbon-bearing Hugin interval and the water-bearing reference zone. The hydrocarbon-bearing response is characterized by a stronger reduction in amplitude toward higher frequencies and a shift toward lower dominant frequency. These observations are consistent with frequency-dependent attenuation and dispersion reported for fluid-sensitive reservoir responses (Castagna et al., 2003; Odebeatu et al., 2006; Ren et al., 2009).

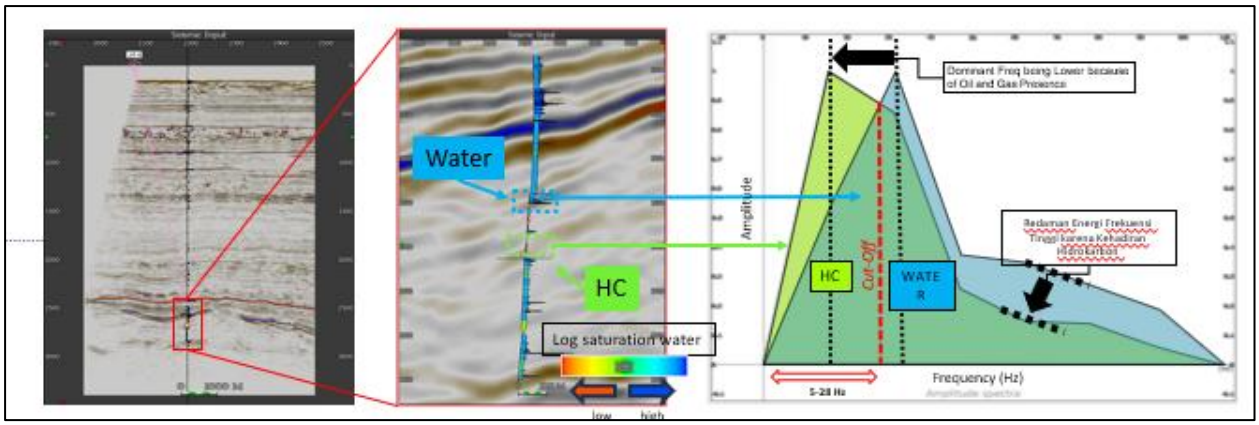


Figure 3. Amplitude–frequency response in hydrocarbon- and water-saturated zones and determination of the cut-off frequency for AVF analysis.

Figure 3 compares the amplitude-frequency responses of the proven hydrocarbon-bearing interval at Well 19-A and the water-bearing reference interval. The hydrocarbon-bearing interval exhibits a relatively stronger amplitude decay toward higher frequencies, while the two spectral responses intersect at approximately 28 Hz. This intersection was used as the upper cut-off frequency, whereas 5 Hz represents the lower bound of the analyzed spectral window. Accordingly, the 5–28 Hz frequency range was consistently used for subsequent AVF regression and attribute generation. Within this interval, the hydrocarbon-bearing reference shows a stronger reduction in amplitude toward higher frequencies compared with the water-bearing response.

Although this spectral contrast is consistent with a fluid-sensitive attenuation response (Odebeatu et al., 2006; Ren et al., 2009), frequency shifts in post-stack seismic data are not uniquely controlled by fluid content. Reservoir thickness and thin-bed tuning can also modify peak frequency and spectral amplitude (Chen et al., 2008). Therefore, the spectral response was not interpreted independently but was further evaluated using SW logs, production information, and an additional validation well.

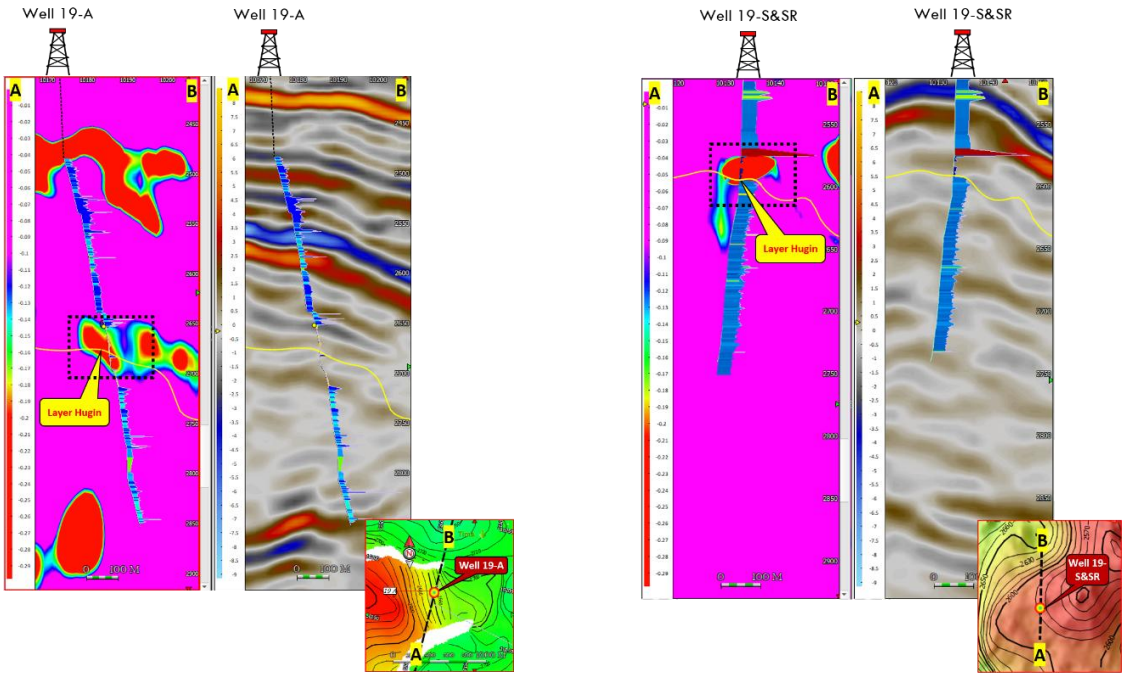
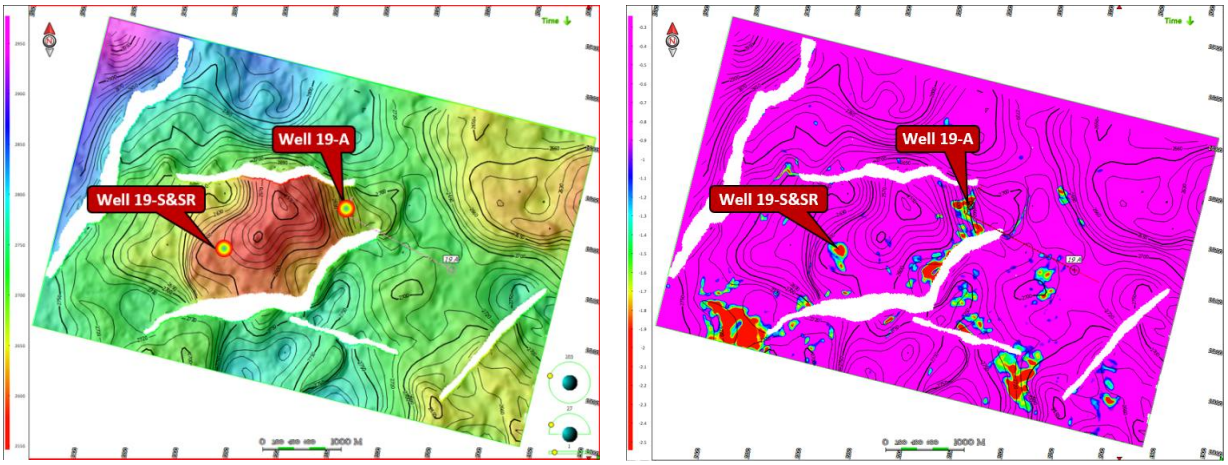


Figure 4. Validation of the AVF response against water saturation (SW) within the Hugin Formation at (a) Well 19-A and (b) Well 19-S&SR.

Figure 4 shows the comparison between the AVF Product response and water saturation (SW) within the Hugin reservoir interval at Wells 19-A and 19-S&SR. At Well 19-A, the reservoir interval is characterized by an SW value of approximately 0.203 and an AVF Product of approximately −0.21. At Well 19-S&SR, the SW decreases to approximately 0.166, while the AVF Product becomes more negative, reaching approximately −0.28. This represents an approximately 18% decrease in SW accompanied by an approximately 33% increase in the magnitude of the negative AVF response. The consistent trend between the two wells indicates that lower water saturation is associated with stronger frequency-dependent attenuation within the analyzed Hugin reservoir interval.

This relationship is consistent with previous studies showing that fluid saturation can influence seismic dispersion, attenuation, and frequency-dependent reflection behavior (Odebeatu et al., 2006; Chen et al., 2008; Ren et al., 2009). The agreement between the AVF Product and SW at two separate wells therefore strengthens the interpretation of the negative AVF response as a fluid-sensitive attenuation anomaly. Nevertheless, because the comparison is based on two validation wells, the observed relationship is regarded as cross-well consistency rather than a statistically established correlation.



(a) (b)

Figure 5. Distribution of the AVF Product attribute within the Hugin Layer interval: (a) structural contour map and (b) AVF Product distribution showing Wells 19-A and 19-S&SR as validation points.

Following calibration at Wells 19-A and 19-S&SR, the AVF Product was mapped across the Hugin Layer to evaluate the lateral distribution of attenuative responses. Figure 5 shows that negative AVF Product anomalies occur around both validation wells and extend laterally within the interpreted Hugin reservoir structure. The anomalies are characterized by relatively strong seismic amplitude accompanied by a negative frequency Gradient, indicating stronger frequency-dependent attenuation (Mandong et al., 2021; Rezeki et al., 2023).

The spatial consistency between the negative AVF response, the Hugin reservoir interval, the structural setting, and the two validation wells strengthens the interpretation of the mapped anomalies as hydrocarbon-prospective zones. The presence of comparable AVF responses at both Wells 19-A and 19-S&SR also indicates that the anomaly is not restricted to a single-well location. Nevertheless, the AVF map is interpreted as a calibrated screening result rather than a definitive fluid map because post-stack frequency responses may also be influenced by reservoir thickness, tuning, lithology, and seismic-data characteristics (Chen et al., 2008).

An important limitation of the present analysis is the potential ambiguity between fluid-related attenuation and tuning-related spectral changes. The Hugin reservoir varies in thickness across the Volve structure, and variations in bed thickness can modify spectral amplitude and

dominant frequency even without changes in fluid content (Chen et al., 2008). Because the present workflow is based on post-stack seismic data, these effects cannot be completely separated from fluid-induced attenuation. Confidence in the interpretation was therefore based on the combined consistency of the AVF response with two well controls, SW information, production history, and structural position rather than on the negative AVF anomaly alone.

The AVF workflow presented in this study also provides a practical example for teaching applied wave physics and geophysics. The analysis connects fundamental concepts of seismic-wave propagation, frequency-dependent attenuation, time-frequency analysis, and fluid–rock interaction with real seismic and well data. In physics or geophysics education, this case study can be used to demonstrate how theoretical concepts such as wave attenuation and spectral decomposition are translated into quantitative subsurface interpretation. The comparison between AVF responses and water saturation at two wells may also support problem-based learning activities in which students evaluate geophysical evidence while considering the non-uniqueness and limitations of seismic interpretation.

4. CONCLUSION

The AVF analysis of the Volve post-stack seismic data identified frequency-dependent attenuation within the Hugin Formation. Spectrum analysis shows a stronger reduction of high-frequency amplitude in the hydrocarbon-bearing reference interval, with the intersection between hydrocarbon- and water-bearing spectral responses occurring at approximately 28 Hz. Accordingly, the 5–28 Hz frequency window was used for AVF regression and attribute generation. The resulting response is characterized by a positive Intercept, negative Gradient, and negative AVF Product, representing stronger frequency-dependent attenuation.

Validation at two wells shows a consistent relationship between AVF Product and reservoir fluid conditions. Well 19-A exhibits an SW of approximately 0.203 and an AVF Product of approximately −0.21, whereas Well 19-S&SR shows a lower SW of approximately 0.166 and a more negative AVF Product of approximately −0.28. The approximately 18% decrease in SW is accompanied by an approximately 33% increase in the magnitude of the negative AVF response, supporting the observed cross-well relationship between lower water saturation and stronger frequency-dependent attenuation. The lateral distribution of negative AVF Product anomalies around both validation wells further supports the delineation of hydrocarbon-prospective zones within the Hugin reservoir.

Nevertheless, the AVF response should not be regarded as a unique indicator of hydrocarbon presence because post-stack spectral behavior may also be influenced by reservoir thickness, thin-bed tuning, lithology, seismic bandwidth, and processing effects (Chen et al., 2008). Therefore, AVF is best used as a calibrated quick-look and screening approach in combination with independent well, geological, and production information rather than as a standalone DHI.

REFERENCES

Biot, M. A. (1956). Theory of propagation of elastic waves in a fluid-saturated porous solid. I. Low-frequency range. Journal of the Acoustical Society of America, 28(2), 168–178. https://doi.org/10.1121/1.1908239

Carcione, J. M., & Picotti, S. (2006). P-wave seismic attenuation by slow-wave diffusion: Effects of inhomogeneous rock properties. Geophysics, 71(3), O1–O8. https://doi.org/10.1190/1.2194512

Castagna, J. P., Sun, S., & Siegfried, R. W. (2003). Instantaneous spectral analysis: Detection of low-frequency shadows associated with hydrocarbons. The Leading Edge, 22(2), 120–127. https://doi.org/10.1190/1.1559038

Chapman, M., Liu, E., & Li, X. Y. (2006). The influence of fluid-sensitive dispersion and attenuation on AVO analysis. Geophysical Journal International, 167(1), 89–105. https://doi.org/10.1111/j.1365-246X.2006.02919.x

Chen, L., Matteucci, G., Fahmy, B., & Finn, C. (2008). Spectral-decomposition response to reservoir fluids from a deepwater West Africa reservoir. Geophysics, 73(6), C23–C30. https://doi.org/10.1190/1.2978337

Conway, G. D., Tröster, C., Scott, B., Hallatschek, K., & ASDEX Upgrade Team. (2008). Frequency scaling and localization of geodesic acoustic modes in ASDEX Upgrade. Plasma Physics and Controlled Fusion, 50(5), 055009. https://doi.org/10.1088/0741-3335/50/5/055009

Greenberg, M. L., & Castagna, J. P. (1992). Shear-wave velocity estimation in porous rocks: Theoretical clastic silicate rock model. Geophysical Prospecting, 40(2), 195–209. https://doi.org/10.1111/j.1365-2478.1992.tb00371.x

Haryanto, H., Sadat, A., & Yusuf, H. (2022). Unlocking shallow play potential by implementing frequency-dependent AVO attribute, East Java Basin. Proceedings of the 47th Annual Scientific Meeting of Himpunan Ahli Geofisika Indonesia (HAGI), Malang, Indonesia.

Innanen, K. A. (2011). Inversion of the seismic AVF/AVA signatures of highly attenuative targets. Geophysics, 76(1), R1–R14. https://doi.org/10.1190/1.3518816

Jicai, J., Sugianto, H., Li, S., Patel, H., & Land, S. (2015). Application of AVF inversion on shale gas reservoir TOC prediction. SEG Technical Program Expanded Abstracts, 3014–3018.

Jin, Z., et al. (2016). Quantitative estimation of gas saturation by frequency-dependent amplitude-versus-offset analysis. Geophysical Prospecting, 64(1). https://doi.org/10.1111/1365-2478.12179

Luo, C., Yuan, S., & Wang, S. (2017). Frequency-dependent reflection coefficients and AVAF inversion for a dispersive reservoir. Journal of Geophysics and Engineering, 14(5), 1167–1176. https://doi.org/10.1088/1742-2140/aa735a

MacBeth, C., Mangriotis, M. D., & Amini, H. (2018). A review of post-stack 4D seismic time-shifts, Part 1: Values and interpretation. Geophysical Prospecting, 66. https://doi.org/10.1111/1365-2478.12688

Mallat, S., & Zhang, Z. (1993). Matching pursuits with time-frequency dictionaries. IEEE Transactions on Signal Processing, 41(12), 3397–3415. https://doi.org/10.1109/78.258082

Mandong, A. F., Bekti, R. P. A., & Saputra, R. I. A. (2021). Amplitude variation with frequency as direct hydrocarbon indicator for quick look and different insight of hydrocarbon delineation. Jurnal Geofisika, 19(2), 62–68. https://doi.org/10.36435/jgf.v20i2.517

Naseer, M. T., & Asim, S. (2017). Continuous wavelet transforms of spectral decomposition analyses for fluvial reservoir characterization of Miano Gas Field, Indus Platform, Pakistan. Arabian Journal of Geosciences, 10, 118. https://doi.org/10.1007/s12517-017-2920-5

Norwegian Petroleum Directorate. (n.d.). Volve. Norwegian Petroleum Directorate/Norwegian Offshore Directorate.

Offshore Technology. (2020). Volve oil field, North Sea. Offshore Technology.

Odebeatu, E., Zhang, J., Chapman, M., Liu, E., & Li, X. Y. (2006). Application of spectral decomposition to detection of dispersion anomalies associated with gas saturation. The Leading Edge, 25(2), 206–210. https://doi.org/10.1190/1.2172314

Partyka, G., Gridley, J., & Lopez, J. (1999). Interpretational applications of spectral decomposition in reservoir characterization. The Leading Edge, 18(3), 353–360. https://doi.org/10.1190/1.1438295

Pelemo-Daniels, D., & Stewart, R. R. (2024). Petrophysical property prediction from seismic inversion attributes using rock physics and machine learning: Volve Field, North Sea. Applied Sciences, 14(4), 1345. https://doi.org/10.3390/app14041345

Pride, S. R., Berryman, J. G., & Harris, J. M. (2004). Seismic attenuation due to wave-induced flow. Journal of Geophysical Research: Solid Earth, 109(B1), B01201. https://doi.org/10.1029/2003JB002639

Purnomo, M. R., Erlangga, M. P., Hafizh, M., & Khoirunas, A. (2025). Intergrasi Seismik Menggunakan Atribut Seismik dan Amplitude Variation with Frequency (AVF) pada Lapangan Penobscot untuk Mengidentifikasi Fluida pada Tight Sand. Jurnal Pendidikan, Sains, Geologi, Dan

Geofisika (GeoScienceEd Journal), 6(4), 2134–2142. https://doi.org/10.29303/goescienceed.v6i4.1537

Raji, W. O., & Rietbrock, A. (2013). Attenuation (1/Q) estimation in reflection seismic records. Journal of Geophysics and Engineering, 10(4), 045012. https://doi.org/10.1088/1742-2132/10/4/045012

Rezeki, D. S. S., Putra, Y. S., Perdhana, R., Arman, Y., & Muhardi. (2023). Penerapan metode amplitude variance frequency pada data seismik daerah reservoir dengan studi kasus Lapangan Teapot USA. Jurnal Geosaintek, 9(1), 8–15. https://doi.org/10.12962/j25023659.v9i1.14005

Ren, H., Goloshubin, G., & Hilterman, F. J. (2009). Poroelastic analysis of amplitude-versus-frequency variations. Geophysics, 74(6), N41–N48. https://doi.org/10.1190/1.3207863

Rutherford, S. R., & Williams, R. H. (1989). Amplitude-versus-offset variations in gas sands. Geophysics, 54(6), 680–688. https://doi.org/10.1190/1.1442696

Saha, S., Vishal, V., Mahanta, B., et al. (2022). Geomechanical model construction to resolve field stress profile and reservoir rock properties of Jurassic Hugin Formation, Volve field, North Sea. Geomechanics and Geophysics for Geo-Energy and Geo-Resources, 8, 68. https://doi.org/10.1007/s40948-022-00359-5

Sen, S., & Ganguli, S. S. (2019). Estimation of pore pressure and fracture gradient in Volve Field, Norwegian North Sea. SPE Oil and Gas India Conference and Exhibition. https://doi.org/10.2118/194578-MS

Sinha, S., Routh, P. S., Anno, P. D., & Castagna, J. P. (2005). Spectral decomposition of seismic data with continuous-wavelet transform. Geophysics, 70(6), P19–P25. https://doi.org/10.1190/1.2127113

Szydlik, T., Smith, P., Way, S., Aamodt, L., & Friedrich, C. (2007). 3D PP/PS prestack depth migration on the Volve Field. First Break, 25, 43–47. https://doi.org/10.3997/1365-2397.25.1106.27412

Taner, M. T., Koehler, F., & Sheriff, R. E. (1979). Complex seismic trace analysis. Geophysics, 44(6), 1041–1063. https:// https://doi.org/10.1190/1.1440994

Wu, X., Chapman, M., Li, X. Y., Angerer, E., & Boston, P. (2014). Quantitative gas saturation estimation by frequency-dependent amplitude-versus-offset analysis. Geophysical Prospecting, 62(6), 1224–1237. https://doi.org/10.1111/1365-2478.12179